Lorentz Force type Self-Bearing Motor for Centrifugal Heart Pump

Yohji Okada #1*
Ibaraki University
Hitachi City, Japan

Tadafumi Miyoshi #2
Ibaraki University
Hitachi City, Japan

Toru Masuzawa #3
Ibaraki University
Hitachi City, Japan

Masato Enokizono #4
Oita University
Oita City, Japan

Ryou Kondo #5
Ibaraki University
Hitachi City, Japan

Abstract

Highly efficient Lorentz force type self-bearing motor is developed. High rotor pole flux density and ampere turns of stator coils are the key technology for strong levitated motor. For this purpose Halbach magnet array and pressed flat coils are used to get high performance. The coil thickness is only 1.6 [mm] with one coil winding of 66 turns. The peak flux density in air gap is about 0.6 [T]. The rotor can run up to 9,000 [rpm] with maximum efficiency over 70 [%]. This self-bearing motor is tried to apply to the centrifugal heart pump.

1 Introduction

The traditional magnetic bearing requires separate AC motor which causes long shaft and low bending vibration [1]. Self-bearing motor had been proposed which had combined functions of magnetic bearing and AC motor. Standard type uses reluctance principle for producing levitation force and Lorentz principle for producing rotation torque. This type has the contradiction between the strong levitation force and rotating torque [1]. For solving this problem the authors has proposed Lorentz type self-bearing motor which produces levitation force and rotation torque both by Lorentz principle [1-7]. In this paper a compact 4 pole outer rotor type Lorentz self-bearing motor is developed. High rotor pole flux density and ampere turns of stator coils are the key technology for strong levitated motor. For this purpose Halbach magnet array on the rotor surface is used to produce high pole flux density. Also the stator is designed to have pressed flat coils to have high cupper ratio with thin air gap [8]. The developed motor produces high levitation force and rotating torque. The servo-motor control is applied to the motor controller based on the measured rotor angle by Hall flux sensors. This produces stable high speed levitated rotation. The results show good performances. Finally the developed motor is tried to apply to the centrifugal artificial heart pump.

2 Principle

The levitation and rotation principle of Lorentz type self-baring motor are shown in Figs. 1 and 2, respectively.

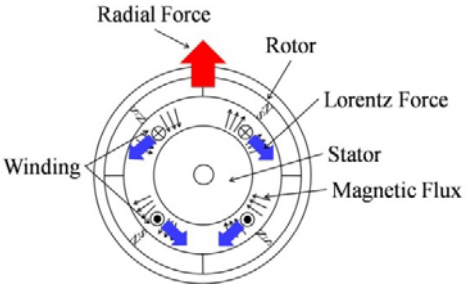

Figure 1: Principle of Levitation

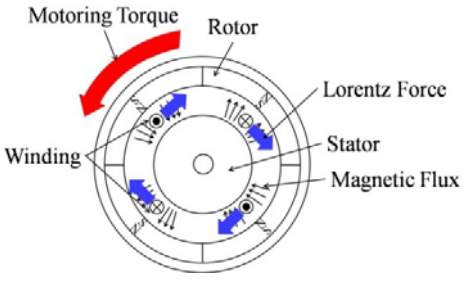

Figure 2: Principle of Rotation

*Contact Author Information: E-mail: y.okada@mx.ibaraki.ac.jp, Address: Ibaraki University, 3-14-6 Nakanarusawa Hitachi Japan, Phone Number: +81-294-38-8033, Fax Number: +81-294-38-5047

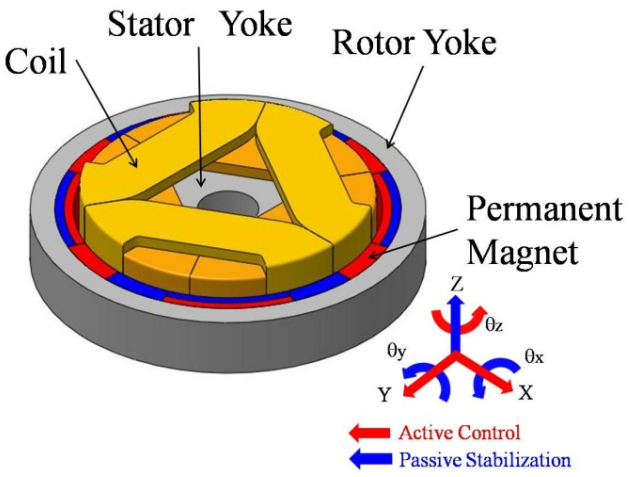

Figure 3: Scheme of Outer Rotor Motor

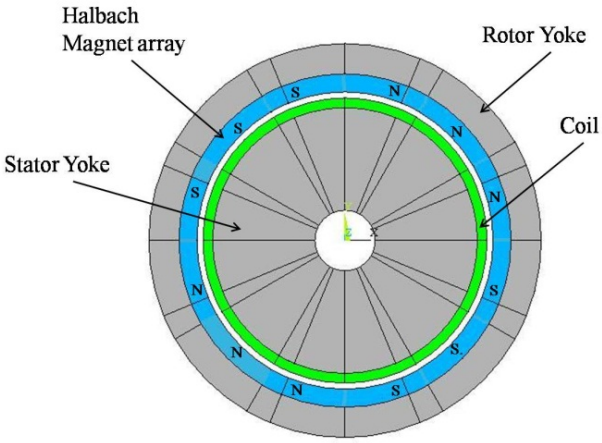

Figure 4: Analytical Model

The figures show surface magnetized 4 pole outer rotor and one pair of coils. The current flows as going into or coming out the surface as shown in Fig. 1, then the Lorentz force acts on the coil downward. The coils are fixed to the stator the reaction radial force acts on the rotor upward. Three phase coils are arranged 60 degrees apart the radial force can be controlled arbitrary magnitude and direction by changing the three phase control currents.

The rotation principle is shown in Fig. 2. The left side coil currents are inversed from the case in Fig. 1, the Lorentz force in the left side is upward while those in the right side is downward. The coils are fixed on the rotor the reaction torque acts on the rotor counter clockwise direction as shown in Fig. 2. The three phase coil currents can control the rotating torque arbitrary.

3 Theoretical Consideration of 4 pole Motor

A 4 pole Lorentz motor is proposed which is expected to reduce the levitation force fluctuation and to have the stronger torque and bearing force. The rotor PMs are assumed to produce the following magnetic flux in the air gap,

$$B_g = B\sin(\omega t + 2\theta) \tag{1}$$

The three phase currents are assumed to flow in each motoring coils. Then the current distribution can be expressed using the Dirac delta function [9]. From the BLI law, the torque can be expressed as,

$$T = 2rl\int_0^{\pi} B_g i_m d\theta = 6rlAB\cos\psi \tag{2}$$

where A and ψ are the magnitude and phase of the three phase motor control current. Hence we can control rotating torque by changing either A or ψ.

Next, let us consider the levitation control. For this purpose we use another three phase coil currents, which is again expressed using the Dirac delta function [9]. Then we have the following radial forces,

$$F_y = \frac{3\sqrt{2}}{2}BCl\cos(\phi - \frac{\pi}{4}) \tag{3}$$

$$F_x = -\frac{3\sqrt{2}}{2}BCl\sin(\phi - \frac{\pi}{4}) \tag{4}$$

where C and ϕ are the magnitude and phase of three phase levitation control current. Hence the magnitude and phase of radial bearing force can be changed by changing C and ϕ.

As a result the levitation can be controlled independently from the motoring control [9].

Items	Values
Outer diameter [mm]	63.2
Rotor yoke thickness [mm]	4.5
PM thickness [mm]	2.5
Mass of rotor [g]	96
Diameter of stator yoke [mm]	44
Air gap (including coil) [mm]	2.6
Coil thickness [mm]	1.6
Coil turn [turns/coil]	66
Yoke axial width [mm]	10

Table 1: Design Parameters

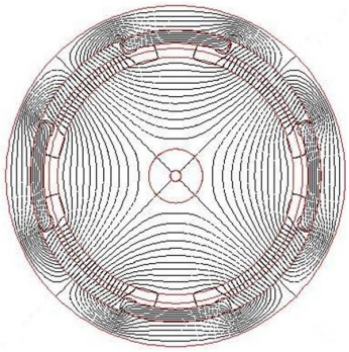

Figure 5: Bias Flux Lines

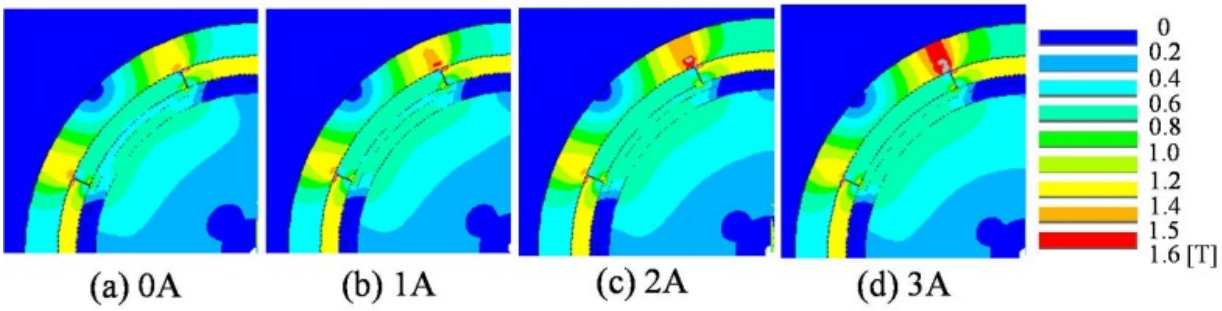

Figure 6: Flux Density Distribution

4 Construction, FEM Analysis and Design

Eight permanent magnets are used and arranged as two segmented Halbach array inside the rotor yoke to produce strong 4 pole flux compared with light rotor weight.

4.1 Construction of Motor

The developed 4 pole motor should have 6 coils, each of which have 90 degree apart going and returning wires. Hence the coil ends are overlapped. Two types of flat pressed coils are manufactured and arranged, the scheme of motor construction is shown in Fig. 3. The coils are made by Selco-coils Co., Ltd [8]. The coils are wound with the rectangular wire of 0.47×0.47 [mm] with 66 turns by pressed manufacturing. The outer rotor has 2 segmented 45 degree PMs. Eight PMs produce 4 pole magnetic flux.

4.2 FEM Analysis and Design

The FEM analysis is carried out by using the model shown in Fig. 4 and the parameters in Table 1. Two dimensional FEM is carried out by trial and error to determine parameters, some of determined them are included in Table 1.

The bias flux lines are shown in Fig. 5. The flux density distributions with the 0 to 3 [A] levitation control current are shown in Fig. 6. The bias flux is well formed. The flux density near 3 [A] control current produces the flux in core close to the saturation level, but the rotor should be light weight we determine to use this rotor.

Finally the bias lux density in air gap, control force and negative force of the rotor are calculated as shown in Figs. 7, 8 and 9, respectively. The figures include experimental results mentioned later. From the calculations the maximum flux density is up to 0.62 [T], the control force factor is about 42 [N/A] and the negative force factor is about 19.5 [kN/m]. They are the value for x-directional calculation. The y-directional control force is about 5 [%] greater, but we consider this difference does not affect critically to levitation control. Even considering the negative force in Fig. 9 the control force in Fig. 8 is strong enough to levitate the rotor.

From the calculated results above we designed the experimental motor. The designed stator parts are shown in Fig. 10 and the designed rotor is shown in Fig. 11.

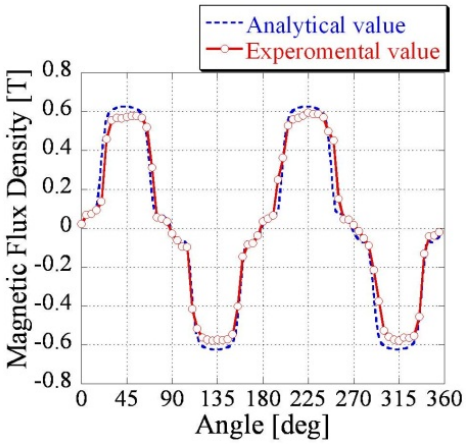

Figure 7: Flux Density in Air Gap

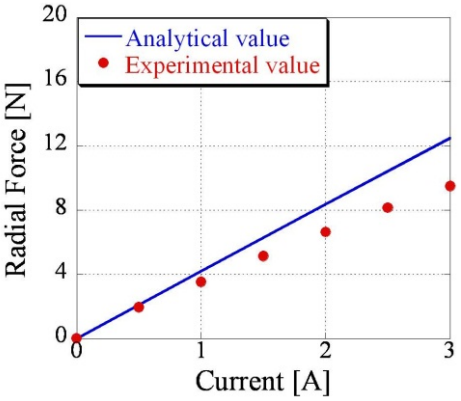

Figure 8: Control Force

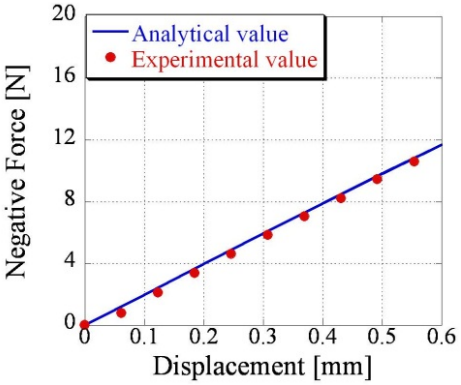

Figure 9: Negative Force

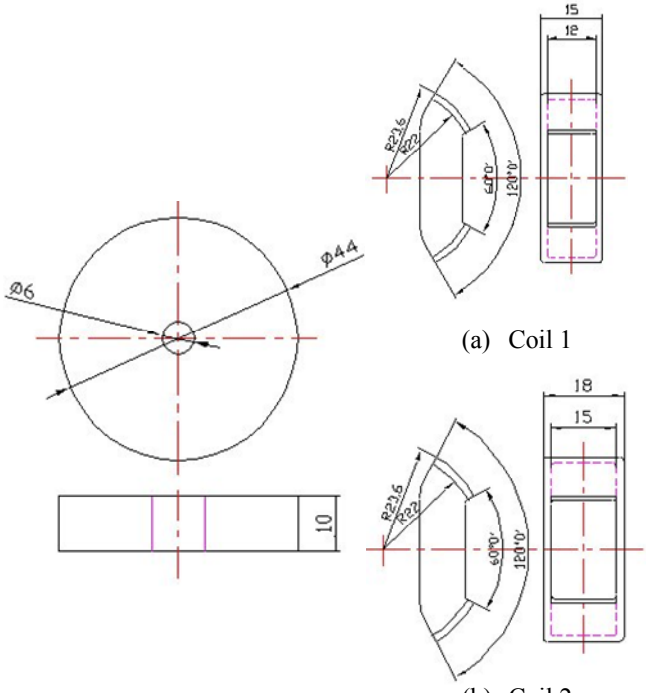

(a) Coil 1

(b) Coil 2

Figure 10: Stator Parts (Left: Back Yoke, Right: Coils)

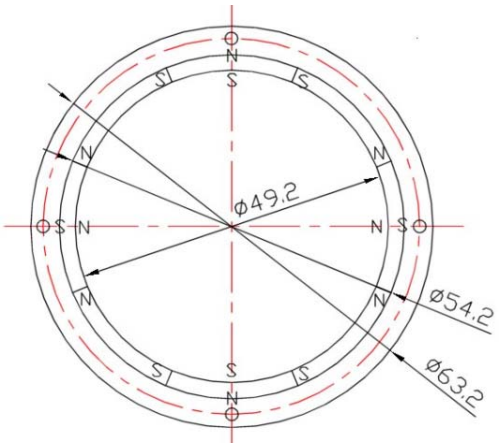

Figure 11: Rotor with 8 PMs

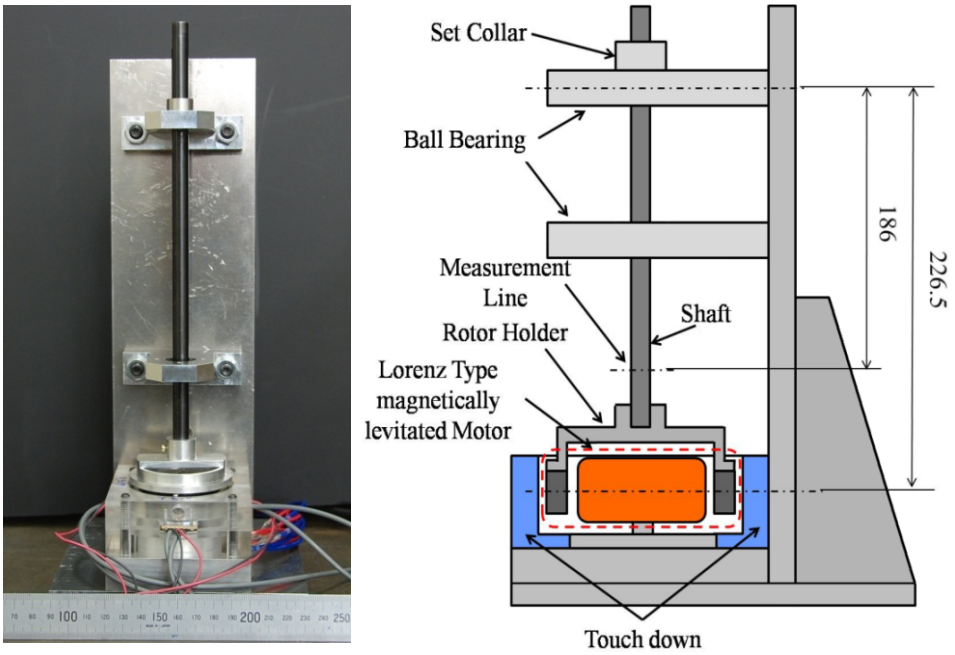

Figure 12: Experimental Setup

5 Experiments

To confirm the performance of above designed motor the experimental setup is fabricated and tested.

5.1 Experimental Setup

The photo (left) and schematic diagram (right) of experimental setup are shown in Fig. 12. This is used to measure the flux density distribution in air gap. Also the radial force and rotating torque characteristics are measured.

5.2 Static Characteristics

The bias flux density in air gap (Fig. 7), control radial force versus current (Fig. 8) and negative force versus displacement (Fig. 9) are measured. The rotor is covered by acrylic touch-down hence the radial displacement and force cannot measure directly at the rotor position as shown in Fig. 12. For this purposes the ball bearing in the middle is removed and the measurement line is marked. The radial displacement and the force are measured at this line. Then they are converted to the values at the rotor position using the distance ratio from the top ball bearing (supporting point) to the measuring point and the rotor position.

The measured flux density distribution is shown by the dots in Fig. 7, where the maximum flux of 0.58 [T] is about 9.4 [%] lower than the calculated value. The measured radial control force is shown by the dots in Fig. 8. The control force factor is about 32 [N/A] which is about 25 [%] lower than the calculation. The measured negative force is shown by the dots in Fig. 9. The negative force factor is about 18.1 [kN/m] which is about 7.4 [%] lower than the calculation.

All the measured values are lower than the calculated values. They are considered that the calculation is carried out using 2-dimensional FEM analysis and the manufacturing has some inaccuracy. We consider these lower measured values are not serious for practical use.

5.3 Levitated Rotation Controller

The previously used controller is the synchronous control algorithm, hence the levitation control is not stable enough [7]. Servo motor control is used based on the measured rotor angle by six Hall sensors (Asahi Kasei HW-322B) as

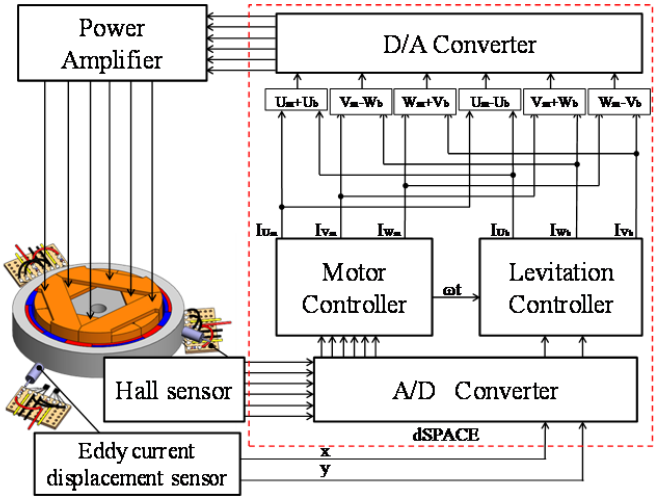

Figure 13: Control System

Parameters	Value
Proportional gain K_P	16.5 [A/mm]
Derivative gain K_D	0.048 [A・sec/mm]
Integral gain K_I	0.28[A/(sec・mm)]
Sampling interval τ	0.1 [msec]
Derivative time constant T_d	0.8 [msec]

Table 2: Control Parameters

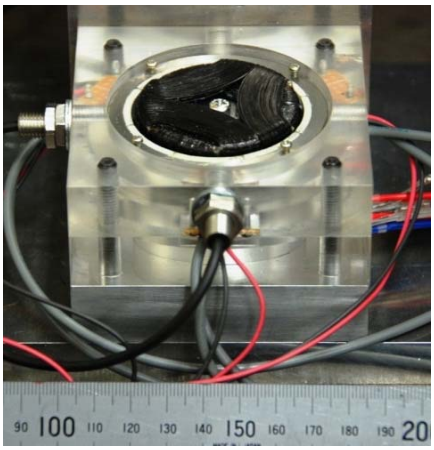

Figure 14: Photo of Levitated Rotation Test Setup

shown in Fig. 13. The resolution of measured electric angle is 7.5 deg. (mechanical angle is 15 deg.) to control levitation and rotation. The digital controller used is installed in dSPACE (DS-1104) with the control parameters listed in Table 2. The each coil current is the addition of the levitation and rotation control currents.

5.4 Experimental Results of Levitation Control

First the levitation control of the rotor is tested. The shaft is removed as shown in Fig. 14. The axial and tilt directions rely on passive stability while the radial two directions are actively controller. The rotor can levitate stably. The impulse response test is carried out. After exciting x-direction by a narrow impulsive signal to the controller, the x and y-directional displacements are measured as shown in Fig. 15. There are some interference between x and y-directions, and the vibration after disturbance is recognized. But the levitation is stable. The case of y-directional excitation gives us similar results and hence it is neglected here.

Next the frequency response is tested. Sinusoidal signal of magnitude ± 0.015 [mm] is added to the controller from the frequency response analyzer (NF FRA5095) and the corresponding response is measured and recorded. The gain and the phase responses of x and y-directions are shown in Figs. 16 and 17, respectively. The resonant peaks on both sides are between 100-150 [Hz]. The peaks are well controlled under 10 [dB].

5.5 Experimental Results of Levitated Rotation

Levitated rotating test is carried out. The orbital trajectories of 2000 [rpm] step are shown in Fig. 18. From these

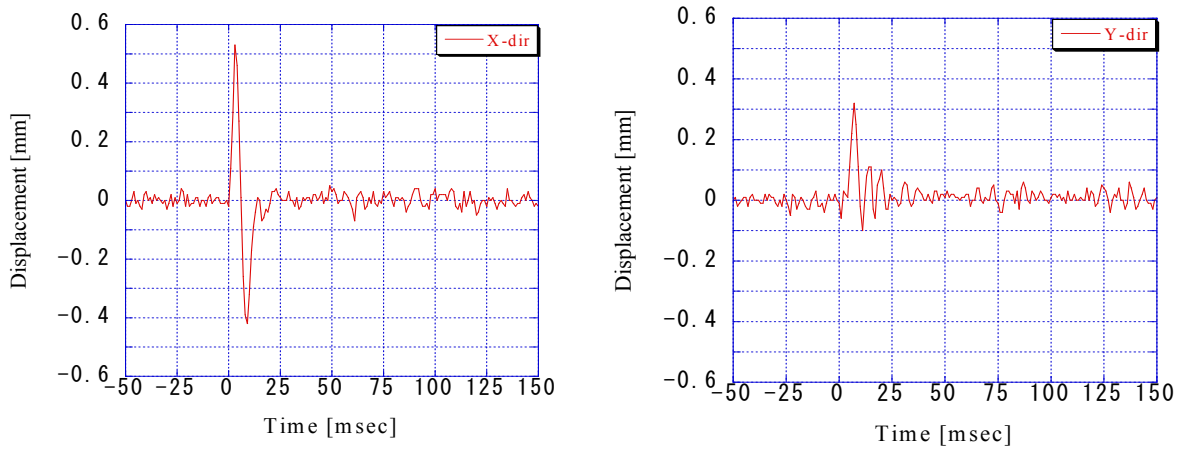

Figure 15: Impulse Response (x-direction excited)

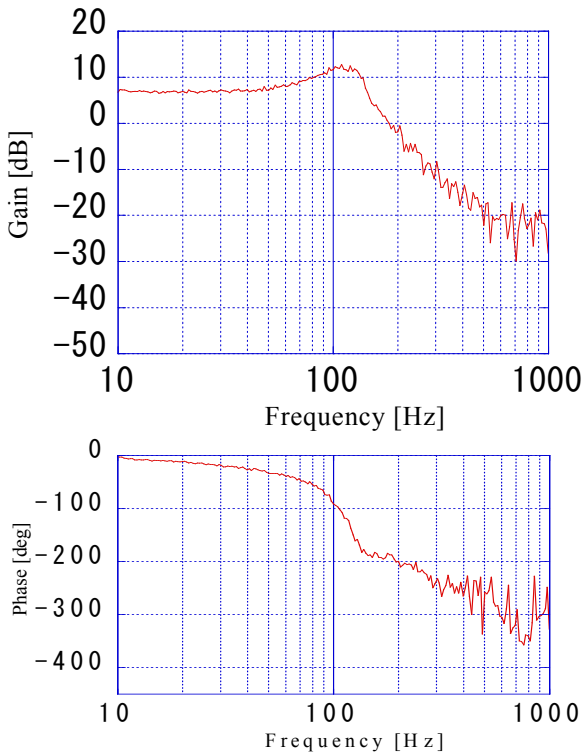

Figure 16: Frequency Response (x-direction)

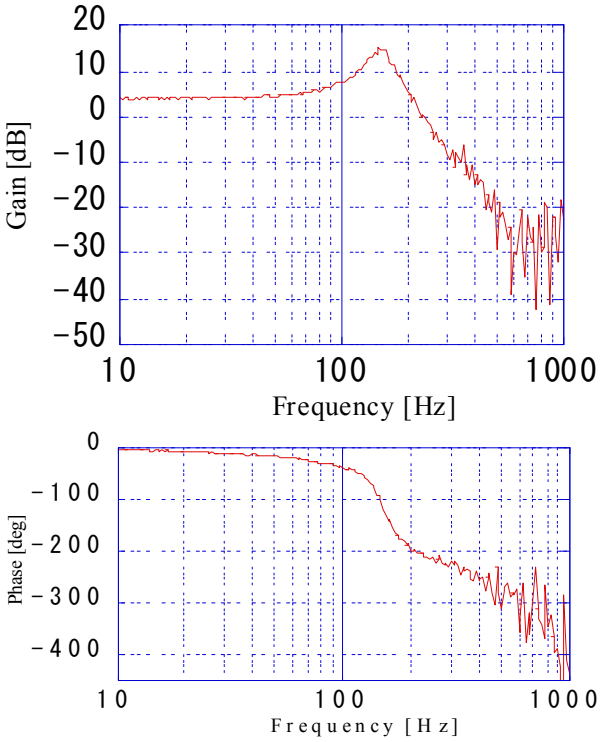

Figure 17: Frequency Response (y-direction)

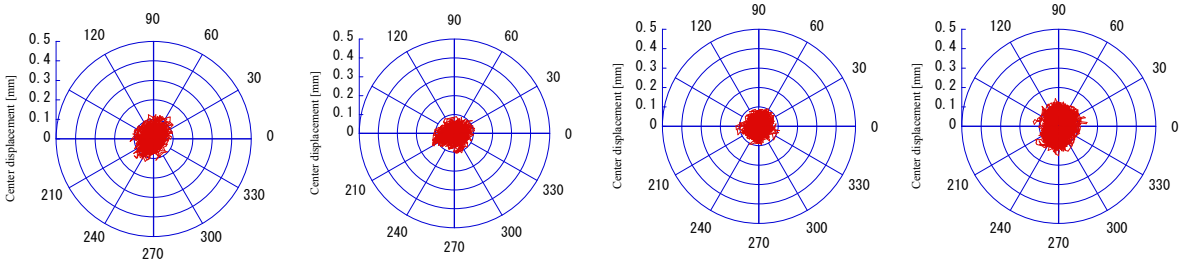

2000 [rpm] 4000 [rpm] 6000 [rpm] 8000 [rpm]

Figure 18: Orbital Trajectory

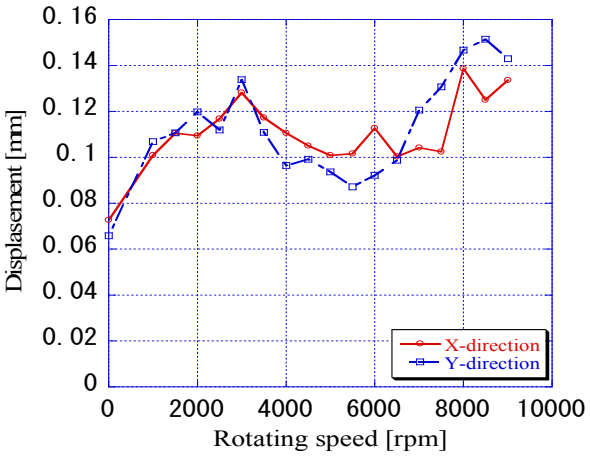

Figure 19: Vibration Amplitude versus Rotation Speed

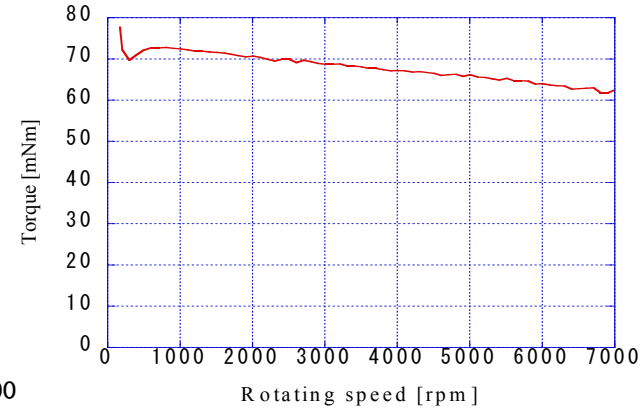

Figure 20: Torque versus Rotation Speed

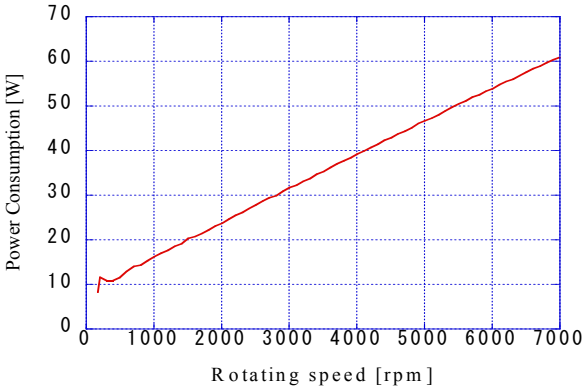

Figure 21: Power Consumption versus Rotation Speed

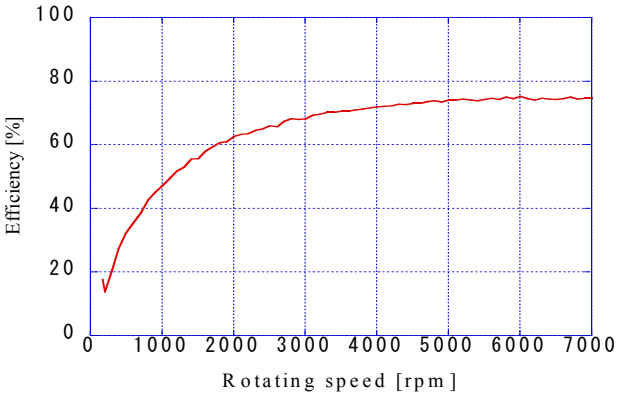

Figure 22: Motor Efficiency versus rotation Speed

orbital trajectories the x and y-directional vibration magnitudes are plotted as shown in Fig. 19. The vibration is increased near 3000 and 8500 [rpm], but they are under the magnitude of ±0.15 [mm] and the rotor can run up to 9000 [rpm]. The stable levitated rotation is confirmed through these experiments.

5.6 Motor Characteristics

The levitated motor characteristics are very difficult to measure with the commercial motor analyzer because the standard motor analyzer is supported by ball bearings. Hence the motor is supported by ball bearings as shown in Fig. 12. Then we measure the motor output torque and speed by motor analyzer (Sugawara PC-SAA2, TB-2KS). The input power is measured by digital power meter (Yokogawa WT1600). Then the output torque, power consumption and the motor efficiency versus rotating speed are calculated as shown in Figs. 20, 21 and 22, respectively. The motor shows relatively high torque about 70 [mNm] compared with its small size. The input power is increased with the rotating speed. The motor efficiency is over 70 [%] while the motor speed is above 3500 [rpm]. These characteristics show relatively good performance for such a small self-bearing motor.

6 Application to Centrifugal Heart Pump

The developed self-bearing motor shows good performance, we try to apply the developed motor to centrifugal artificial heart pump. The prototype pump is made of acrylic acid resin, we need to increase the air gap from 1 [mm] to 1.5 [mm]. Only the rotor diameter is increased; the inner diameter is from 49.2 to 50.2 and the outer diameter is from 63.2 to 64.2 [mm]. The thickness of permanent magnet and back yoke are the same. The stator and the Hall effect sensors are also the same. Photo of developed heart pump is shown in Fig. 23. However we could not get

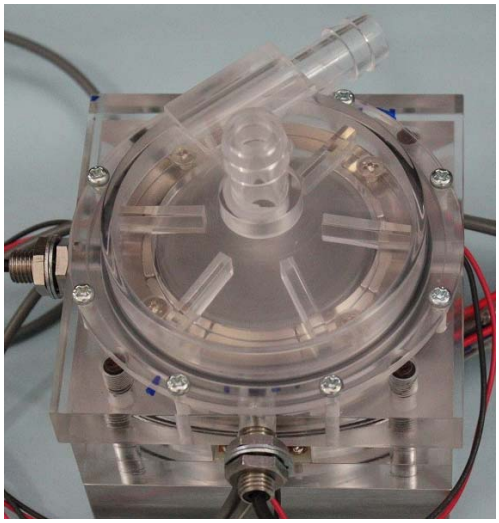

Figure 23: Photo of centrifugal artificial heart pump

good levitated rotation yet. The main reasons are the increase of the air gap and the manufacturing inaccuracy. Still we are working to improve the levitated rotation. After we get good levitated rotation, we will measure the pump performance.

7 Conclusions

High performance self-bearing motor is proposed and developed. The developed motor has the outer diameter of 63.2 [mm] and the core thickness of 10 [mm] which produced high motor torque over 70 [mNm], and high efficiency about 70 [%]. The levitated rotating test is very stable and the motor can run up to 9000 [rpm]. The developed self-bearing motor is tried to apply to the centrifugal heart pump. We are still working on this heart pump. The results may be reported near future.

Acknowledgement

The research is supported by the Grant-in Aid for Science Research (B)(1), under Project Number 20360106. The authors would appreciate Mr. K. Isagawa for his cooperative work.

References

[1] Okada, Y., Self-Bearing Motors. In Schweitzer, G. and Maslen, E. H., editors, *Magnetic Bearings*, Springer, Heidelberg, pp. 461—476, 2009.

[2] Jinbu, T. and Okada, Y., Lorentz type Self-bearing Motor, Transaction of JSME, Ser. C, Vol. 70, No. 698, pp. 2791-2796, 2004 (in Japanese).

[3] Okada, Y., Konishi, H., Kanebako, H. and Lee, C. W., Lorentz Force type Self Bearing Motor, *Proc. of 7th Int. Symp. on Magnetic Bearings*, Zurich, pp. 353-358, 2000.

[4] Stephens, L. S. and Kim, D. G., Force and Torque Characteristics for a Slotless, Lorentz Self Bearing Motor, *IEEE Transactions on Magnetics*, Vol. 38, pp. 1764-1773, 2002.

[5] Park, S.-H., Lee C.-W. and Okada, Y., Design of Lorentz Force type Integrated Motor-Bearing System Using Permanent Magnets and Concentrated Windings, *Proc. of 11th World Congress in Mechanism and Machine Science*, Tianjin, China, pp. 1-5, 2003.

[6] Okada, Y., Kitagou, M., Masuzawa, T. and Enokizono, M., Development of Flux Concentrated type Self-Bearing Motor, *Proc. of 2010 IFAC Symposium on Mechatronics*, Sept. 12-15, Cambridge, MA, USA.

[7] Okada, Y., Isagawa, K., Kitagou, M., Masuzawa T. and Onokizono, M., Small sized Lorentz type Self-Bearing Motor, *Proc. of 19th MAGDA Conference in Sapporo*, pp. 57-60, 2010 (in Japanese).
[8] Selco-coils, Co. Ltd., http://www.selco-coil.com/.
[9] Okada, Y., Jinbu, T., Yamamoto, N. and Sagawa, K., Lorentz type Self-Bearing Motor using Halbach Magnets, *Proc. of 10th Int. Symp. on Magnetic Bearings*, Martigny Switzerland, 2006.